

PERFORMANCE LIMITATIONS IN SUBBAND ACOUSTIC ECHO CONTROLLERS

¹Rhonda J. Wilson, ²Patrick A. Naylor, ²D. Mike Brookes

¹Meridian Audio Limited
Huntingdon, Cambridgeshire

²Dept. of Electrical and Electronic Engineering
Imperial College, London, UK.

ABSTRACT

This paper investigates performance limitations in subband acoustic echo controllers due to modelling errors. It is shown that the subband model of a system is exact only when the number of taps in each subband filter is infinite. When the number of taps used is finite, it is shown that the system modelling error represents an upper bound on performance.

1. INTRODUCTION

In this paper the analysis given by Gilloire and Vetterli [1] is extended for the special case in which the model matrix is made to be diagonal, as shown in Fig. 1. The subband filters are derived from the solution to the Wiener-Hopf equations in each subband for the case of stationary unit variance white noise input. This derivation yields analytic expressions for the modelling error. Subsequently, a direct relationship is derived between the coefficients of the optimal subband filters of a given order and the equivalent full-band system. From this, it is shown that general full-band systems can only be modelled by a subband FIR system using filters of infinite order in each band.

Simulation results are given which show the effect of the modelling error when the system is a unit delay and when the system is that of a typical handsfree telephone.

2. SUBBAND MODELLING

The formulation of Gilloire and Vetterli is adopted from [1] where it is shown that, for a two subband system, the general form of the subband filters in a structure similar to that shown in Fig. 1 is the model matrix

$$\mathbf{C}_m(z) = \begin{bmatrix} C_{0,0}(z) & C_{0,1}(z) \\ C_{1,0}(z) & C_{1,1}(z) \end{bmatrix}, \quad (1)$$

Using (1) and defining $\mathbf{H}(z) = \begin{bmatrix} H_0(z) & H_0(-z) \\ H_1(z) & H_1(-z) \end{bmatrix}$,

$\mathbf{S}(z) = \begin{bmatrix} S(z) & 0 \\ 0 & S(-z) \end{bmatrix}$ and $\mathbf{X}(z) = \begin{bmatrix} X(z) \\ X(-z) \end{bmatrix}$, then

$\mathbf{C}_m(z)$ is derived in [1], so as to give zero subband error signals, from the solution of

$$\mathbf{C}_m(z^2)\mathbf{H}(z) = \mathbf{H}(z)\mathbf{S}(z). \quad (2)$$

In fact, the system shown in Fig. 1 is a special case of great practical interest in which the model matrix $\mathbf{C}_m(z)$

is diagonal such that $C_{00}(z) = C_0(z)$, $C_{11}(z) = C_1(z)$, $C_{01}(z) = C_{10}(z) = 0$.

Choosing

$$H_0(z) = H(z) \text{ and } H_1(z) = H(-z) \quad (3)$$

it is shown [1] that either of the following conditions must be true in order for the solution of (2) to yield a zero error using a diagonal model matrix:

$$H_0(z)H_1(z) = 0 \text{ or } S(z) - S(-z) = 0. \quad (4)$$

We define a signal $\hat{x}(n)$ which is the component of $e(n)$ due only to $x(n)$ when $S(z) = 0$. Using the conditions of (3) to obtain alias cancellation, the z -transform of $\hat{x}(n)$ can be written

$$\hat{X}(z) = -\frac{1}{2} \left[X(z) \left(H^2(z)C_0(z^2) - H^2(-z)C_1(z^2) \right) + X(-z) \left(H(z)H(-z)C_0(z^2) - H(z)H(-z)C_1(z^2) \right) \right] \quad (5)$$

for which terms in $X(-z)$ vanish if at least one of the following conditions is true:

$$H(z)H(-z) = 0 \quad (6)$$

$$C_0(z^2) - C_1(z^2) = 0, \quad (7)$$

otherwise, aliasing occurs. From (4), (5), (6) and (7), the problems of subband adaptive filtering can be summarized:

- Aliasing will be generated unless ideal filter banks are used, or the unknown system $S(z)$ is even, or the subband adaptive filters are identical in each band.
- The accuracy of subband modelling is limited because the subband filtering is a function of z^2 whereas the unknown system S is a function of z . Hence, for a general $S(z)$ which cannot be assumed even, $S(z)$ can only be approximated by the subband adaptive filters. This approximation error is present even if no aliasing is generated.

3. DERIVATION OF THE SUBBAND FILTERS

3.1 Expressions in z for the optimal subband filters.

If we consider the case when $\mathbf{C}_m(z)$ is forced to be diagonal as shown in Fig. 1 the adaptive filtering can then be expressed in terms of a search for $C_0(z)$ and $C_1(z)$ which, in the limit, satisfy $Y_0(z) - \hat{Y}_0(z) = 0$ and

$Y_1(z) - \hat{Y}_1(z) = 0$ respectively over the band of frequencies from $-\pi$ to π . The resulting expressions are

$$C_0(z) = \frac{\begin{pmatrix} H_0(z^{1/2})S(z^{1/2})X(z^{1/2}) + \\ H_0(-z^{1/2})S(-z^{1/2})X(-z^{1/2}) \end{pmatrix}}{H_0(z^{1/2})X(z^{1/2}) + H_0(-z^{1/2})X(-z^{1/2})} \quad (8)$$

$$C_1(z) = \frac{\begin{pmatrix} H_1(z^{1/2})S(z^{1/2})X(z^{1/2}) + \\ H_1(-z^{1/2})S(-z^{1/2})X(-z^{1/2}) \end{pmatrix}}{H_1(z^{1/2})X(z^{1/2}) + H_1(-z^{1/2})X(-z^{1/2})}$$

These can be simplified when $X(z) = X(-z)$ and $H_0(z)$, $H_1(z)$ are ideal lowpass and highpass filters respectively, then

$$C_0(z) = S(z^{1/2}) \quad \text{and} \quad C_1(z) = S(-z^{1/2}). \quad (9)$$

3.2 Derivation of optimal subband filters from solutions to the Wiener-Hopf equations.

For the structure shown in Fig. 1, the subband filters, $C_0(z)$ and $C_1(z)$, which optimally model the system $S(z)$ are now derived from solutions to the Wiener-Hopf equations. The analysis filters $H_0(z)$ and $H_1(z)$ are chosen to be perfect linear-phase half-band lowpass and highpass filters respectively so that no aliasing is generated by decimation by 2, i.e.

$$\begin{aligned} h_0(n) &= \frac{1}{2} \text{sinc}(n\pi/2), \\ h_1(n) &= (-1)^n \frac{1}{2} \text{sinc}(n\pi/2), \end{aligned} \quad (10)$$

$n = -\infty, \dots, \infty.$

The signals $x'_0(n)$ and $y_0(n)$ in Fig. 1 are given by

$$x'_0(n) = \frac{1}{2} \sum_{k=-\infty}^{\infty} \text{sinc}(k\pi/2)x(2n-k) \quad (11)$$

$$y_0(n) = \frac{1}{2} \sum_{k=-\infty}^{\infty} \text{sinc}(k\pi/2)d(2n-k)$$

When $x(n)$ is unit variance white noise, the autocorrelation function $r_0(m)$ of the signal $x'_0(n)$ can be found by writing

$$\begin{aligned} r_0(m) &= E[x'_0(n)x'_0(n+m)] \\ &= E\left[\left(\frac{1}{2} \sum_{k=-\infty}^{\infty} \text{sinc}(k\pi/2)x(2n-k)\right) \times \right. \\ &\quad \left. \left(\frac{1}{2} \sum_{l=-\infty}^{\infty} \text{sinc}(l\pi/2)x(2(n+m)-l)\right)\right] \\ &= \begin{cases} 0 & \text{for } m \neq 0 \\ \frac{1}{2} & \text{for } m = 0 \end{cases} \end{aligned} \quad (12)$$

and therefore the autocorrelation matrix $\mathbf{R} = \frac{1}{2}\mathbf{I}$.

The crosscorrelation of $x'_0(n)$ and $y_0(n)$ is given by

$$p(i) = E[x'_0(n-i)y'_0(n)], \quad (13)$$

$$\mathbf{p} = \frac{1}{2} \begin{bmatrix} \sum_{q=0}^Q \text{sinc}((q-2I_0)\pi/2)s_q \\ \vdots \\ \sum_{q=0}^Q \text{sinc}(q\pi/2)s_q \\ \vdots \\ \sum_{q=0}^Q \text{sinc}((q-2I_M)\pi/2)s_q \end{bmatrix}$$

where the subband filter $C_0(z)$ has coefficients over the range I_0 to I_M with I_0 allowed to be negative. The system $S(z)$ has impulse response $\mathbf{s} = [s_0, s_1, \dots, s_Q]$. The solution of the Wiener-Hopf equation $\mathbf{c}_0 = \mathbf{R}^{-1}\mathbf{p}$ yields the subband filter which minimises the mean square output error for a given system $S(z)$ and a given range of the filter indices I_0 and I_M as

$$c_{0_i} = \sum_{q=0}^Q \text{sinc}((q-2i)\pi/2)s_q, \quad I_0 \leq i \leq I_M \quad (14)$$

and similarly

$$c_{1_i} = \sum_{q=0}^Q (-1)^q \text{sinc}((q-2i)\pi/2)s_q, \quad I_0 \leq i \leq I_M. \quad (15)$$

3.3 Modelling Error.

We now consider the minimisation of the tap norm by writing

$$\hat{\mathbf{c}} = \hat{\mathbf{c}}_0 + \hat{\mathbf{c}}_1. \quad (16)$$

$\hat{\mathbf{c}}_0$ is the equivalent full-band filter corresponding to the path through an ideal analysis filter, decimator, arbitrary lower subband filter, interpolator and ideal synthesis filter. $\hat{\mathbf{c}}_1$ is the equivalent full-band filter corresponding to the path through an ideal analysis filter, decimator, arbitrary upper subband filter, interpolator and ideal synthesis filter. The coefficients of $\hat{\mathbf{c}}_0$ and $\hat{\mathbf{c}}_1$ can be written as

$$\hat{c}_{0j} = \frac{1}{2} \sum_{i=I_0}^{I_M} c_{0i} \text{sinc}((j-2i)\pi/2) \quad (17)$$

and

$$\hat{c}_{1j} = \frac{1}{2} \sum_{i=I_0}^{I_M} c_{1i} (-1)^j \text{sinc}((j-2i)\pi/2). \quad (18)$$

The resulting full-rate impulse response has coefficients

$$\hat{c}_j = \frac{1}{2} \sum_{i=I_0}^{I_M} (c_{0i} + (-1)^j c_{1i}) \text{sinc}((j-2i)\pi/2). \quad (19)$$

The squared tap norm can be written

$$\begin{aligned} \|s - \hat{c}\|^2 &= \sum_{j=-\infty}^{\infty} (s_j - \hat{c}_j)^2 = \sum_{j=0}^Q s_j^2 - 2 \sum_{j=0}^Q s_j \hat{c}_j + \sum_{j=-\infty}^{\infty} \hat{c}_j^2 \\ &= \sum_{j=0}^Q s_j^2 - \sum_{j=0}^Q s_j \sum_{i=I_0}^{I_M} \left((c_{0i} + (-1)^j c_{1i}) \times \right. \\ &\quad \left. + \frac{1}{2} \sum_{m=I_0}^{I_M} (c_{0m}^2 + c_{1m}^2) \right) \text{sinc}((j-2i)\pi/2) \end{aligned} \quad (20)$$

To find the minimum squared tap norm, partial derivatives of (20) with respect to each filter coefficient can be taken and set to zero. This leads precisely to equations (14) and (15), which were derived by minimising the output error.

It is now possible to write an expression for the equivalent full-band filter which corresponds to subband filtering using optimal subband filters of a given length by substituting (14) and (15) into (19) giving

$$\hat{c}_j = \frac{1}{2} \sum_{i=I_0}^{I_M} \sum_{q=0}^Q s_q \{1 + (-1)^{q+j}\} \text{sinc}((q-2i)\pi/2) \text{sinc}((j-2i)\pi/2). \quad (21)$$

When j is even and q is odd $\{1 + (-1)^{q+j}\}$ equals zero. When j and q are even and $I_0 \leq 0$ and $I_M \geq Q/2$,

$$\hat{c}_j = \frac{1}{2} \sum_{q=0}^Q s_q \{1 + (-1)^q\} \text{sinc}((q-j)\pi/2) = s_j. \quad (22)$$

When j is odd and q is even the terms within the braces of (22) sum to zero. When j and q are odd,

$$\hat{c}_j = \sum_{q=0}^Q s_q \sum_{i=I_0}^{I_M} \text{sinc}((q-2i)\pi/2) \text{sinc}((j-2i)\pi/2). \quad (23)$$

We now determine the limits of i for which $\hat{c}_j = s_j$, j odd. This can be found by using

$$\begin{aligned} &\sum_{\substack{i=-\infty \\ q \text{ odd} \\ j \text{ odd}}}^{\infty} \text{sinc}((q-2i)\pi/2) \text{sinc}((j-2i)\pi/2) \\ &= \sum_{i=-\infty}^{\infty} \text{sinc}((q-i)\pi/2) \text{sinc}((j-i)\pi/2) - (1)^2 = 1 \end{aligned} \quad (24)$$

since $q-j$ is always even when both q and j are odd, and since

$$\sum_{\substack{i=-\infty \\ q \text{ odd} \\ j \text{ odd}}}^{\infty} \text{sinc}((q-i)\pi/2) \text{sinc}((j-i)\pi/2) = \begin{cases} 1 & \text{if } q=j \\ 0 & \text{otherwise} \end{cases}. \quad (25)$$

Hence the range of coefficient indices in the subband filters $I_0 = -\infty$, $I_M = +\infty$, $I_0 \leq i \leq I_M$ yields $\hat{c}_j = s_j$, j odd.

This analysis shows that the optimal subband system with at least $Q/2$ taps in each of two subbands will model perfectly the even taps of $S(z)$, such that

$$\hat{c}_j = \frac{1}{2} (c_{0i} + c_{1i}) = s_j \quad \text{for } j = 2i, 0 \leq i \leq Q/2. \quad (26)$$

It also shows that the optimal subband system can model the odd taps of $S(z)$ perfectly if an infinite number of taps is used in each of the two subbands, from equations (19) and (23), such that

$$\hat{c}_j = \frac{1}{2} \sum_{i=-\infty}^{\infty} (c_{0i} - c_{1i}) \cdot \text{sinc}((j-2i)\pi/2) = s_j. \quad (27)$$

4. SIMULATIONS AND RESULTS

The aim of the first experiment is to investigate the two sources of errors in subband system identification, namely, aliasing error due to non-ideal filter banks and modelling error as highlighted in this paper. The unknown system $S(z) = z^{-1}$.

In this experiment, the filter banks use the designs of Johnston [2] for 16-tap, 32-tap and 64-tap filters, and further designs based on the same criteria for 128-tap and 256-tap filters. Within each subband, optimal subband filters given by (16) and (17) are applied. The number of taps in the subband filters is varied using $I_0 = -[1,2,4,8,16,32,64,128,256,512]$ and $I_M = -I_0 - 1$. For each filter bank order and for each subband filter order, the signal $e(n)$ in Fig. 1 is used to compute the mean square error normalised to the desired response $d(n)$ and averaged across five trials using Gaussian distributed white noise input signals. These results are plotted in Fig. 2 which also shows the theoretical modelling error, $\|s - \hat{c}\|^2 / \|s\|^2$, for ideal filter banks.

The key features of Fig. 2 are as follows.

(a) The accuracy of a subband model of $S(z) = z^{-1}$ is generally very poor even for subband filters of up to 1024 taps in each subband.

(b) The theoretic result shows an upper bound on the accuracy of the subband model which increases with the number of taps in each subband.

The second experiment used USASI noise as the input signal and the system response was the measured 2048-tap response of a handsfree telephone. The analysis and synthesis filters were the all-pass polyphase filters described in [3]. The two band system was run with

$I_0 = [0, 2, 4, 8, 16, 32, 64, 128]$ and $I_M = 1023$, for 32000 samples of the input signals with an exact initialization FTF-GMC algorithm [4] used in each of the subbands. Fig. 3 shows the theoretical modelling error and the final normalised mse as a function of subband length. The theoretical modelling error reduces from -17dB to -29dB with increasing subband filter length. When there is no output measurement noise the normalised mse reduces from -42dB to -44dB. When SNR is 40dB the normalised mse reduces from -37.8dB to -38.5dB. When the input signal is correlated minimising the output error does not minimise the modelling error; the difference between the theoretical modelling error and the measured normalised output error indicates that the adaptive subband system has been able to obtain good output error reduction even when the modeling error is large

When a system is undermodelled (as is the case when subband filters are used) the system which minimises the output error for one correlated signal will not necessarily minimise the output error for another correlated signal. The improvement in the theoretical modelling error as the subband filter length is increased indicates that this is beneficial to ensure that low output error is obtained for non-stationary signals such as speech.

5. CONCLUSIONS

The observation that full-band adaptive systems, as used in system identification or acoustic echo control, can obtain significantly smaller final misadjustment than subband systems with the same number of adaptive parameters motivated this study of modelling errors in subband adaptive filters. An explanation has been presented for the difference in final misadjustment which suggests that the modelling capability of subband systems is limited not only by aliasing errors due to non-ideal filter banks but also by the intrinsic properties of the subband structure.

6. REFERENCES

- [1] A. Gilloire and M. Vetterli, "Adaptive filtering in subbands with critical sampling: Analysis, experiments, and applications to acoustic echo cancellation," *IEEE Trans. Signal Processing*, vol. 40, pp. 1862-1875, Aug. 1992.
- [2] R. E. Crochiere and L. R. Rabiner, *Multirate digital signal processing*. Englewood Cliffs, NJ: Prentice-Hall, 1983.
- [3] J. E. Hart, P. A. Naylor and O. Tanrikulu, "Polyphase allpass IIR structures for sub-band acoustic echo cancellation," in *Proc. EUROSPEECH'93*, 1993, pp. 1813-1816.
- [4] R. J. Wilson "Noise Source Cancellation in Audio Recordings", PhD Thesis, Imperial College, London 1997.

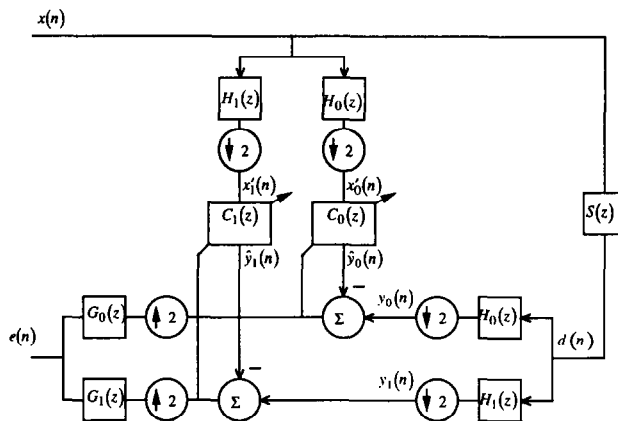


Fig. 1. Subband structure.

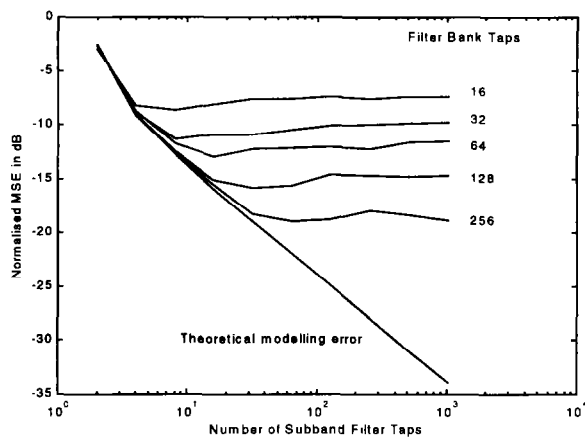


Fig. 2. Normalised mean square error as a function of subband filter length for filter bank lengths of 16, 32, 64, 128 and 256, and the theoretical modelling error for $S(z) = z^{-1}$.

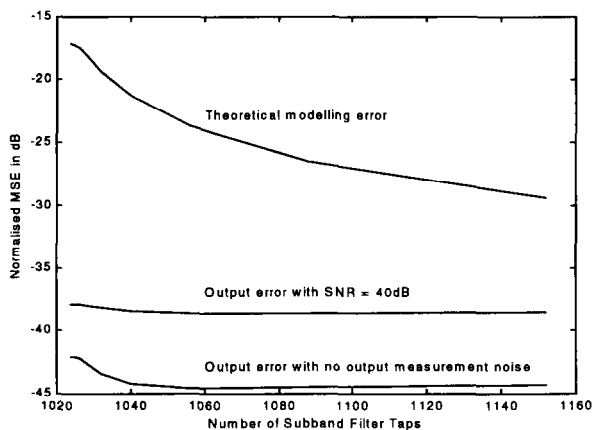


Fig. 3. Normalised mean square output error when SNR is 40dB and when there is no measurement noise, and the theoretical modelling error as a function of subband filter length for the system of length 2048.